KTH Aeronautical
and Vehicle Engineering

Acoustics of parallel baffles muffler with Micro-perforated panels

By

Xiaowan Su

MSc thesis in Technical Acoustics

Stockholm 2011-10-06

KTH Report TRITA AVE 2011:84

Abstract

Micro-perforated panels (MPP) have a good acoustic damping performance and a potential to be used in mufflers [1, 2]. This thesis aims to investigate the acoustic performance of a parallel baffles muffler, which consists of MPP baffles. The work is both experimental and numerical, i.e., a model is developed for a MPP baffles muffler with local reaction. The prototype MPP mufflers tested in the thesis were all produced by the Swedish company Sontech.

First, the experiments were based on the procedure for experimental characterization of heat exchangers described in Ref. [5]. The transmission loss and flow generated sound are tested at four flow speeds for seven kinds of parallel baffles.

Second, the mathematical modeling is built on the basis of the standard models of a locally reacting liner muffler [13]. The impedance for the Micro-perforated panels is computed using the models described by Maa [1] and Guo [2].

Acknowledgement

Thanks to my principle supervisor Professor Mats Åbom for your kind guidance and help. I am grateful for being able to learn so much from you.

Thanks to my second supervisor Dr. Sabry Allam, who gave me the main support and courage throughout this thesis.

Thanks to Lars Wester from Sontech, who gave the opportunity to take apart in this thesis and for supplying the test objects.

Also thanks to Danilo Prevelic, who helped me for all measurements with nice a mood.

Finally, I want to thank to my friends in Stockholm, thank you for your encourage and patience throughout this thesis.

List of symbols

Symbol	Quantity	Dimension
c_o	Sound speed in air 343m/s at 20 C^0	m/s
d	Diameter of the width of slits	m
f	Frequency	Hz
h	Length of slit	m
j	Imaginary unit	
k	Perforate constant	
k_o	Wave number	
p^+	Incident wave pressure complex valued amplitude	Pa
p^-	Reflected wave pressure complex valued amplitude	Pa
p_i	Pressure at microphone i complex valued amplitude	Pa
q_i	Volume velocity at microphone i complex valued amplitude	m^3/s
t	Thickness of the sample	m
u	Particle velocity inside holes or slits complex valued amplitude	m/s
r	Normalized resistance	
wm	Normalized reactance	
Z_P	The entire normalized impedance of a MPP plate	
M	Mach number	
α	End correction coefficient of resistance	
Δp	Sound pressure difference between the ends of the tube	Pa
η	Dynamic viscosity	Kg/(m.s)
ω	Angular frequency	Rad/s
ρ_o	Density of air	Kg/m^3
σ	Perforation ratio	
μ	Kinematic viscosity	m^2/s

Contents

1. Introduction ... 1
    1.1 Definition of Acoustics Impedance ... 1
    1.2 Micro-perforate panel ... 1
    1.3 Parallel baffles muffler with Micro-perforated panel ... 2
2. Measurement methods ... 4
    2.1 The theory of the measurement method ... 4
        2.1.1 Measurements without flow ... 4
        2.1.2 Measurements with flow ... 4
    2.2 Measurement equipment setup ... 7
3 Measurement results and analysis ... 10
    3.1 Test samples ... 10
        3.1.1 The MPP baffles ... 10
        3.1.2 Inclined (=I) parallel baffles mufflers ... 11
        3.1.3 Straight (=S) parallel baffles mufflers ... 13
    3.2 The experimental results ... 15
        3.2.1 The transmission loss of the tested mufflers ... 15
        3.2.2 The flow noise (ISO 3746:1995) ... 19
        3.2.3 The comparison of different test samples ... 22
        3.2.4 Pressure drops ... 26
4. Models of parallel baffles muffler with locally reacting wall impedance ... 27
        4.1 The geometry of the model ... 27
        4.2 The theoretical formulation of the model: ... 28
    4.3 The modeling results ... 30
        4.3.1 The transmission loss ... 30
        4.3.2 The comparison of modeling and experiments ... 32
5. Summary and conclusions ... 34
References ... 35

1. Introduction

1.1 Definition of Acoustics Impedance

Mathematically, it is a ratio between a complex valued pressure and a complex valued velocity component at a certain sound field point. The ratio is called the specific acoustic impedance and is given by:

$$Z_S = \frac{\hat{p}}{\hat{u} \cdot n} \qquad (1)$$

$\hat{p}$ is the pressure; $\hat{u}$ is the velocity, n is a unit vector.

The impedance is a complex quantity:

$$Z = R + iX \qquad (2)$$

where R is the real part of the impedance, which is referred to as resistance; X is the imaginary part, which is referred to as reactance.

The dimensionless normalized impedance is also widely used, which can be calculated using the following equation:

$$z = \frac{Z}{\rho c} \qquad (3)$$

where Z is the impedance; ρc is the air impedance.

1.2 Micro-perforate panel

A Micro Perforated Panel (MPP) is a device, which can be used to absorb sound and reduce its sound intensity. The structure of the MPP is quite simple, consisting of a thin flat plate, which is normally 0.5-2 mm thick, with small holes or slits drilled or punched in it. The diameter of the hole or the width of the slit is in the sub-millimeter range [1]. The Micro-Perforated Panel absorber depends on its characteristic impedance, which can by itself provide enough high acoustic normalized resistance (around 1) and low acoustics mass reactance, without additional fibrous or other porous materials. Because the thickness of the micro-perforate panel is very thin, the velocity between two sides will be the same. So the impedance can be calculated using the following equation:

$$Z = \frac{\Delta \hat{p}}{\hat{u} \cdot n} \qquad (4)$$

where $\Delta \hat{p}$ is the pressure difference across the MPP, $\hat{u}$ is the velocity, n is the unit vector. There are three main acoustic dissipation mechanisms: linear and nonlinear for no flow conditions, and the grazing flow for flow conditions. The linear mechanism consists of two parts: internal and external. The mechanism of the internal part is to convert the acoustic energy into heat via viscosity, which only has effects on the resistance. The mechanism of the external part consists of surface resistance related to surface viscous dissipation. The nonlinear part is caused by high sound intensity which will create acoustic induced vorticity and even a jet at very high amplitudes. The acoustic resistance will increase with the increasing particle velocity inside the MPP holes. The third mechanism is the grazing flow effect. The resistance will increase with grazing flow [2].

1.3 Parallel baffles muffler with Micro-perforated panel

The parallel baffle mufflers based on a porous material are used extensively in heating, ventilation and air conditioning systems for increased attenuation of noise [3]. This kind of dissipative silencer can also be used for attenuating broadband noise emanating from fluid moving devices, such as internal combustion engines and cooling fans. The structure of the parallel baffles muffler is simple. The parallel baffles muffler consists of a series of rectangular shaped bodies, which are made of porous material and for protection often enclosed in a metallic frame with perforated sides. But the porous material has its own drawbacks- the limitation of fatigue life and working atmosphere for example. In this thesis the baffle body will be only made of Micro-perforated panels (see figure 2). The inside structure of the baffle body can be empty or filled with a rigid walled core preventing sound propagation inside the baffles. The acoustical performance of a parallel baffle muffler can be described by determining the transmission loss. The effect of the baffle muffler comes from reflection of sound at the inlet and outlet cross-sections and from damping along the baffle. Normally except for low frequencies the damping along the baffle is the dominating effect. The reflection will depend on the open area of the baffle arrangement (see figure 1). The damping will depend on the surface impedance of the baffles, which is affected by the MPP impedance and the interior of the baffle, and the baffle length.

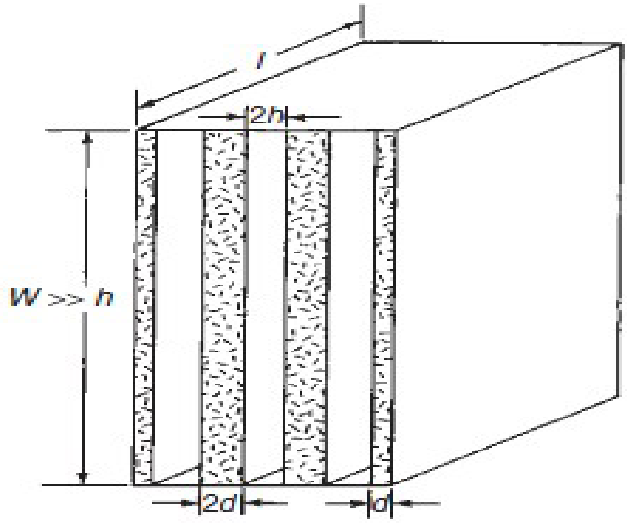

Figure 1: A parallel baffles muffler [6] with flow and sound propagating between baffles. The open area ratio is given by h/d.

Figure 2: A parallel baffles muffler with Micro-perforated panels.

2. Measurement methods

The measurements are designed to investigate the performance of the parallel baffles muffler's acoustic characteristics, here represented by the sound transmission loss and flow generated noise of the muffler for different flow rates. For the flow cases the sound transmission loss was determined using a modified ISO standard procedure (ISO 15186- 1:2000). The sound power was determined using a standard ISO procedure with a reference source (ISO 373: 2000) [4].

2.1 The theory of the measurement method

The method of transmission lost measurement is the diffuse sound field based on the ISO 15186-1:2000 [3, 5], which is standard for testing sound reduction of wall elements.

In the real case, the sound field incident is an unknown mix of waves and incidence angles. So it is assumed that the device (parallel baffles muffler) can be regarded as a wall element which here will be tested using a random ("diffuse") type of sound field.

2.1.1 Measurements without flow

The two acoustics rooms are connected by a wall, where a parallel baffles muffler is inserted. A sound source emitting broad noise was positioned in the reverberation room, see Figure 3. The sound reduction index (or transmission lost) can be measured in the receiving room, anechoic room, with ISO 15186-1:2000 [3, 5]:

$$R_I = L_{P_I} - \left(L_{I_I} + 10\log(Sm/S)\right) - 6 \tag{5}$$

The sound pressure level, L_P, can be measured by a rotating microphone in the reverberation room. The sound intensity level, L_I, is obtained by scanning the surface of the parallel baffles muffler with an intensity probe in the receiving anechoic room; Sm is the total area of the measurement; S is the area of the test specimen under test. In our case Sm can be regarded as equal to S. So the sound reduction equation can be calculated using the following equation:

$$R_I = L_{P_I} - L_{I_I} - 6 \tag{6}$$

2.1.2 Measurements with flow

A measurement with flow (from the anechoic to the reverberation room) will not fulfill the ISO standard procedure. So it needs two modifications to calculate the sound transmission loss.

The first modification is to find out the difference (for no flow) of the transmission lost when measured in the "wrong" direction, i.e., from the anechoic room to the reverberation room, see Figure 4. This difference is called the correction factor, which can be used to correct the measurements with flow. The sound reduction can be calculated by following equation:

$$R_{II} = L_{PAII} - L_{prII} \qquad (7)$$

The sound pressure level, L_{PAII}, can be measured by three fixing microphones one meter way from the muffler in anechoic room. The sound pressure level, L_{PRII}, can be measured by a rotating microphone in reverberation room.
The first correction factor can be calculated by the following equation:

$$A = R_{II} - R_{I} \qquad (8)$$

The sound reduction R_I can be calculated by equation 6 and the sound reduction R_{II} can be calculated by equation 7.

The second modification is to investigate the effect of flow generated sound. The noise of flow-generated sound can be tested by the microphones in both acoustic rooms, see Figure 5, and be subtracted as background noise in the actual measurement.

In the final measurement, there are sound sources and flow coming from the anechoic room, see Figure 6. The sound pressure levels in both rooms can be tested by the microphones. The measured sound pressure levels cannot be used directly, but should be corrected by the two modifications discussed above. First, the flow-generated sound is eliminated. Then the sound transmission can be calculated using the following equation:

$$R_{final} = R_{III} - A \qquad (9)$$

R_{final} is the standard transmission loss; R_{III} is the transmission loss which is corrected for flow noise; A is the correction factor, calculated by equation 8.

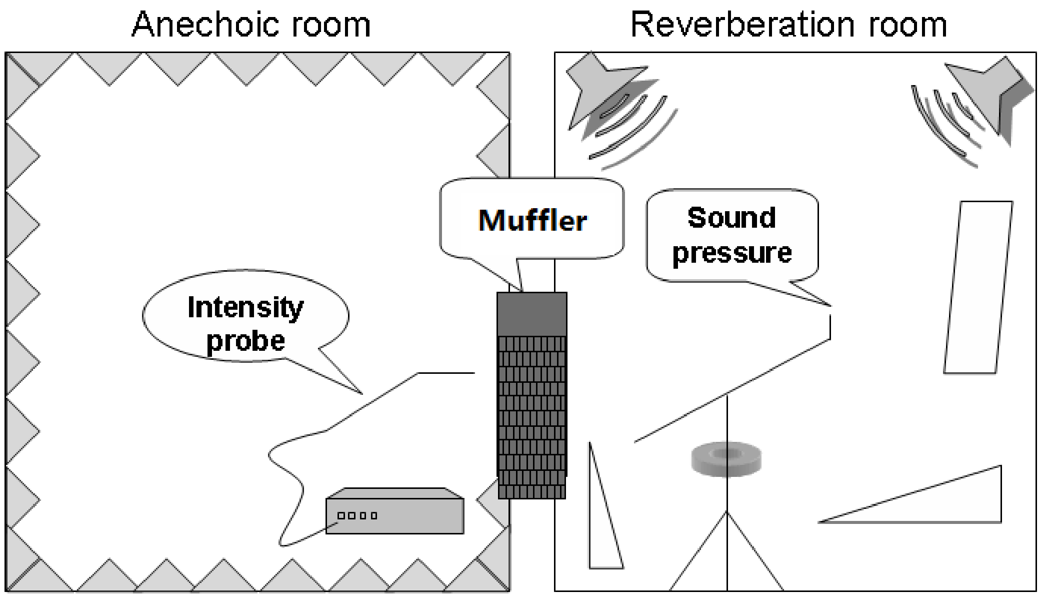

Figure 3: The standard transmission loss measurement without flow.

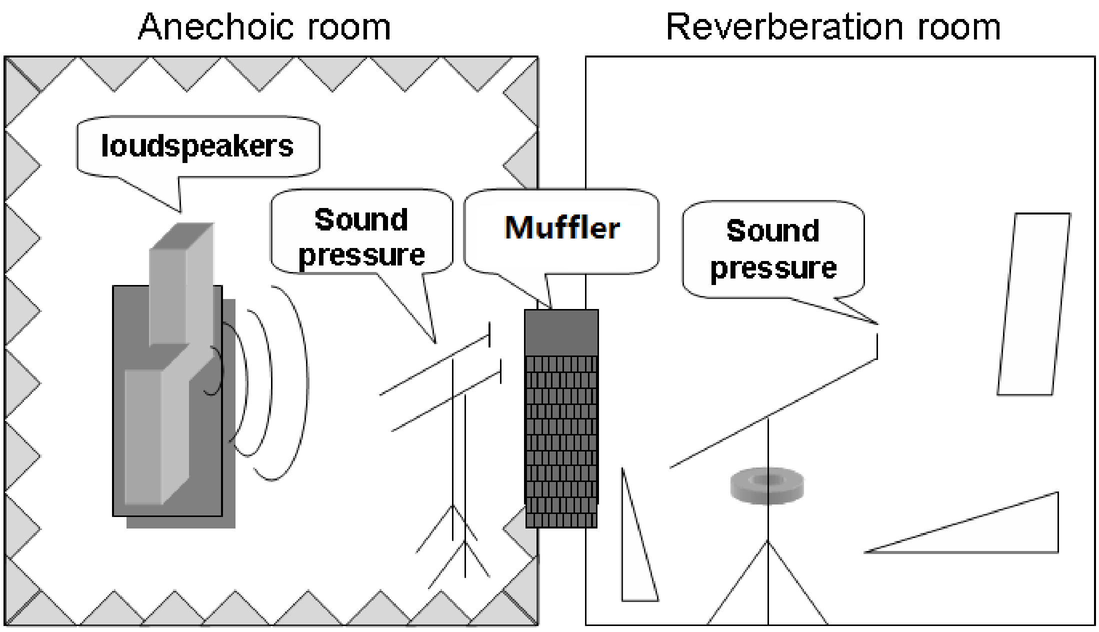

Figure 4: The first modification measurement.

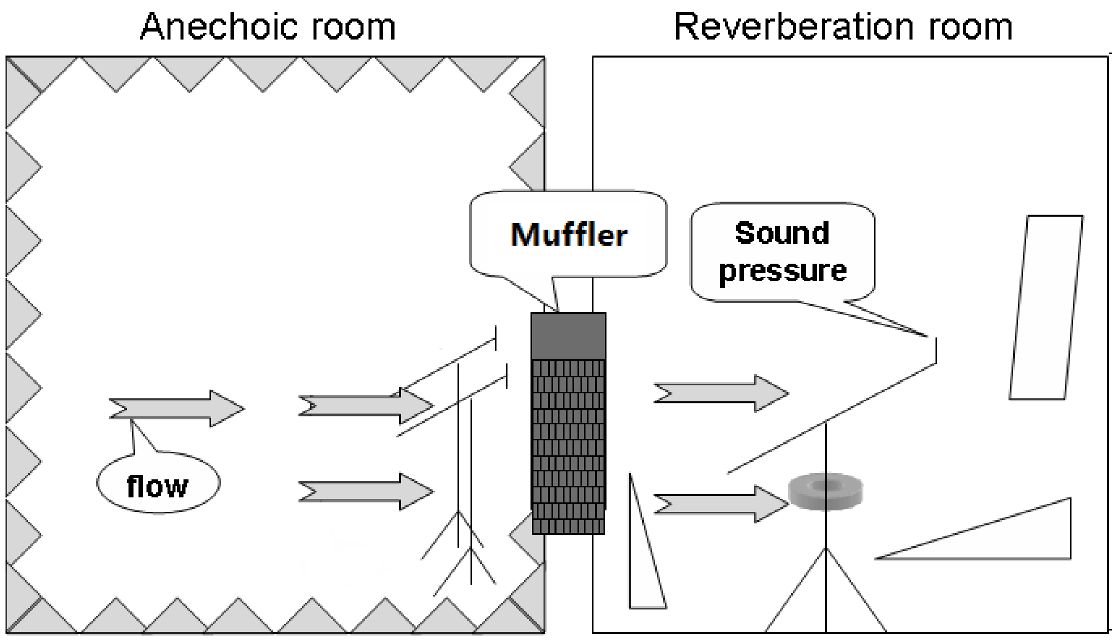

Figure 5: The second modification measurement.

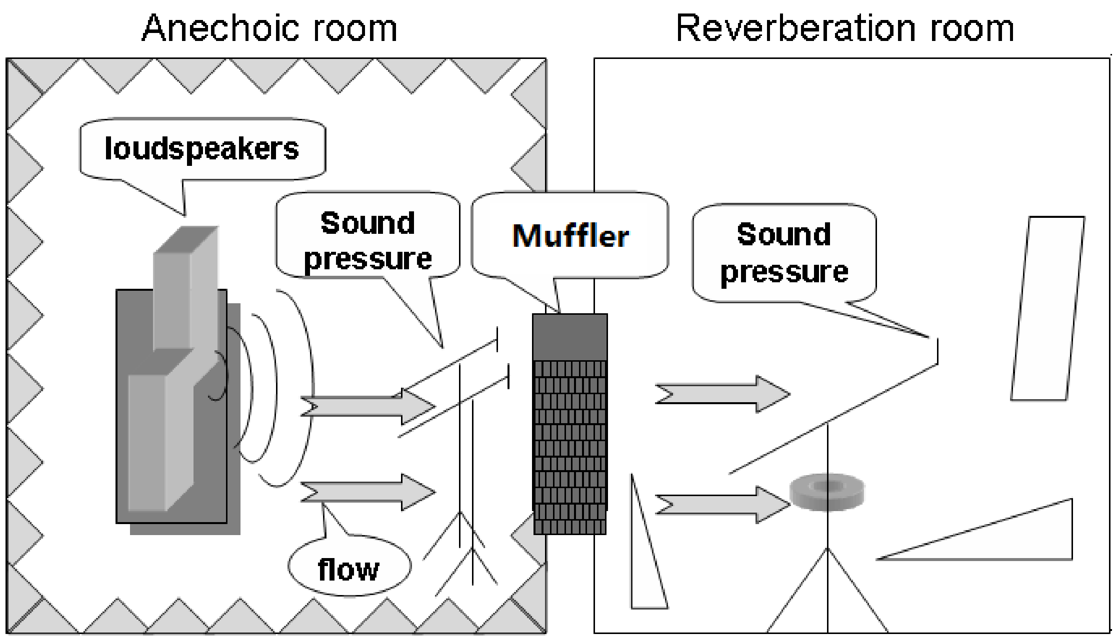

Figure 6: The final measurement with flow.

2.2 Measurement equipment setup

The whole setup of the measurement can be seen in the Figure 7. The seven test cases (baffles types & arrangements) were fixed in the wall between the reverberation room and anechoic room. The frame of the test objects are attached to a short duct made of sheet metal, see Figure 8. The test equipment used is shown in Figure 9.

(a) (b)

Figure 7: The setup for the measurement (a) Anechoic room (b) Reverberation room.

Figure 8: The frame of the test samples.

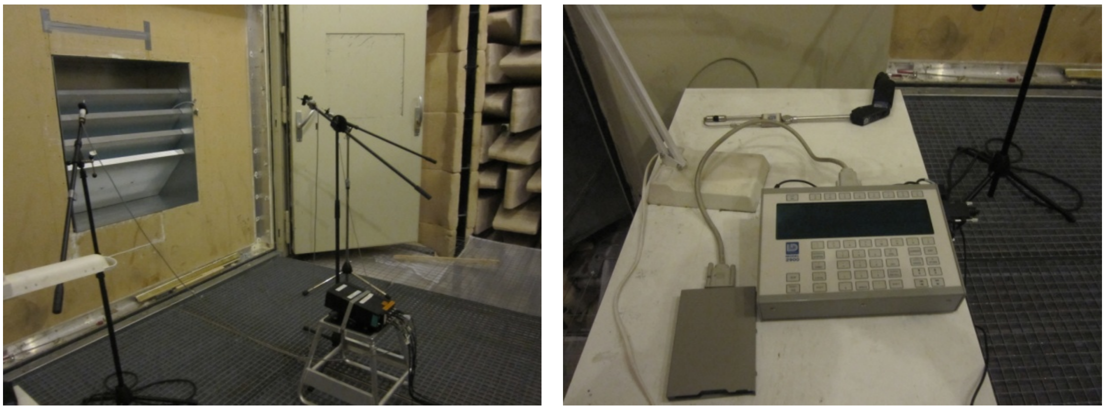

Figure 9: The microphones and intensity probe.

Figure 10: The process of fixing baffles.

3 Measurement results and analysis

3.1 Test samples

Figure 11: Photo of the test MPP (Acustimet^{TM}) with slits used to build the MPP baffles.

Thickness t (mm)	Slit width d (mm)	Porosity (%)
1	0.25	1

Table 1: The dimension of the MPP with slits.

3.1.1 The MPP baffles

All test samples consist of parallel baffles mufflers, see Figure 12. The dimension of the Micro-perforated panel baffle, in front, is shown in Figure 13 and Table 2.

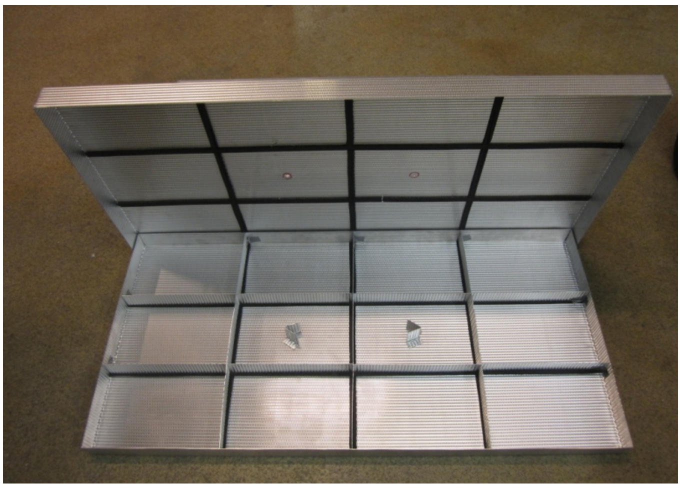

Figure 12: Photo of the MPP baffle with inner rigid walls. Another type with an empty interior was also tested.

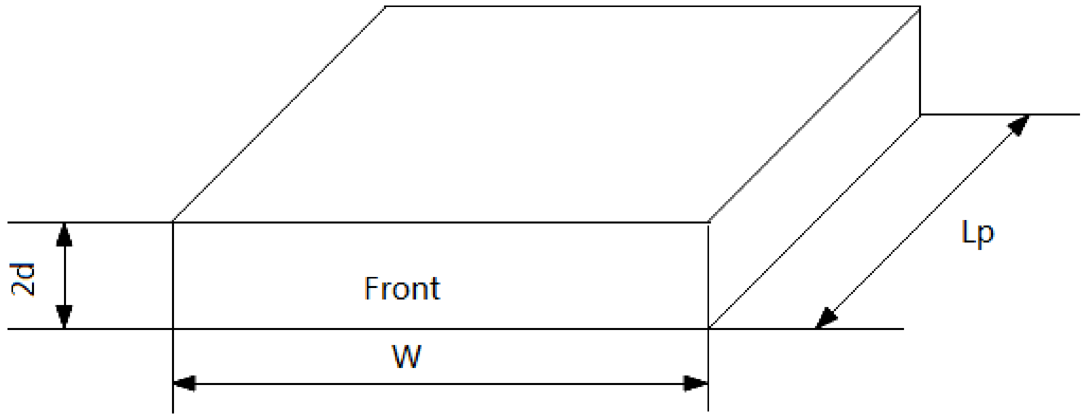

Figure 13: The dimensions of one MPP baffle.

Width 2d (mm)	Length W (mm)	Lp (mm)
50	980	497

Table 2: The dimensions of the MPP baffle.

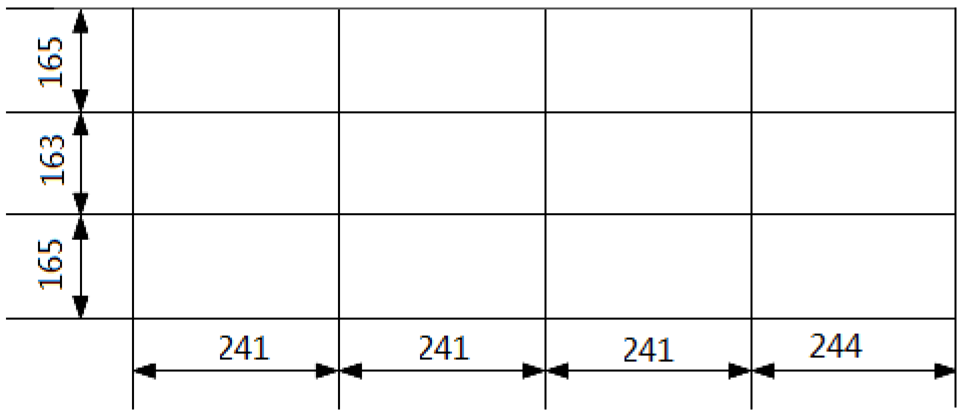

Figure 14: The dimensions of the rigid inner wall mesh in mm.

3.1.2 Inclined (=I) parallel baffles mufflers

The I6 parallel baffles muffles consist of six MPP baffles, see Figure 15. The six MPP baffles are all with inner rigid walls. And all of them are fixed in an inclined angle, 30 degree, and the certain distance. There is a cover on the top of the muffler in the reverberation room side, which is used to keep the muffler sealed, i.e., to avoid an open area.

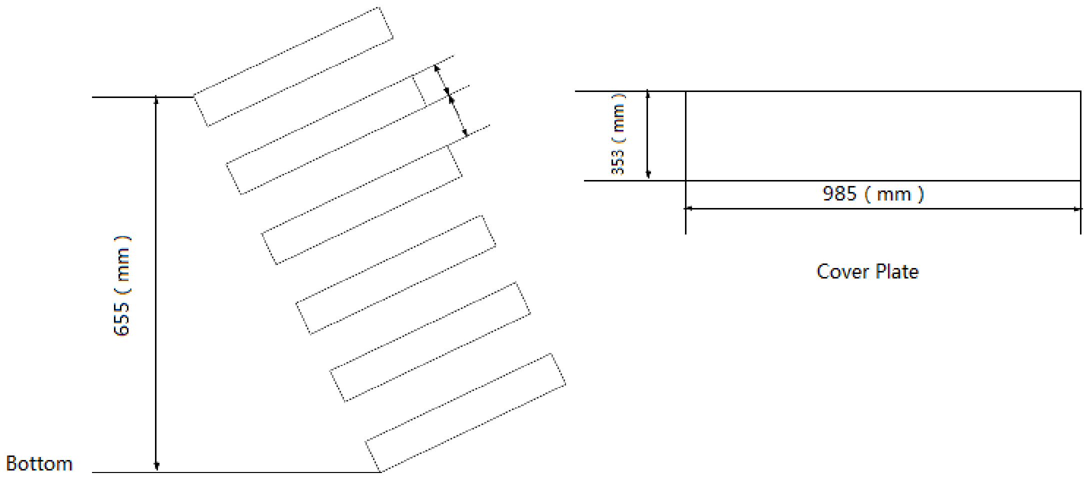

Figure 15: The dimension of the I6 sample.

Number	The width of the baffle d(m)	The air channel distance h(m)	Fixing angle
6	0.025	0.0265	30^{o}

Table 3: The dimension of I6 baffles muffle.

I4 parallel baffles muffler

The I4 parallel baffles muffles consist of four MPP baffles, see Figure 16. The baffle design details are the same as for the I6 case. The dimension of the whole muffler is shown in the Figure 17, see also table 4.

(a) (b)

Figure 16: Photo of the I4 sample (a) Anechoic room (b) Reverberation room

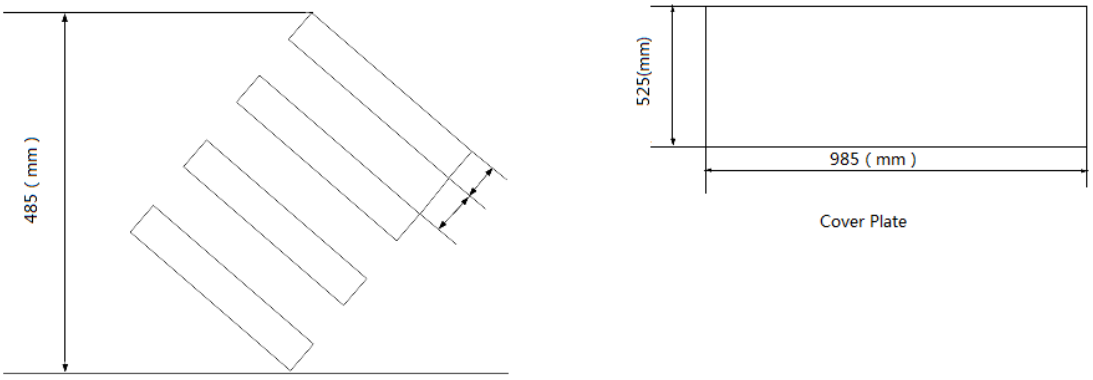

Figure 17: The dimension of the I4 sample.

Number	The width of the baffle d(m)	The air channel distance h(m)	Fixing angle
4	0.025	0.0265	45^{o}

Table 4: The dimension of I4 baffles muffler.

3.1.3 Straight (=S) parallel baffles mufflers

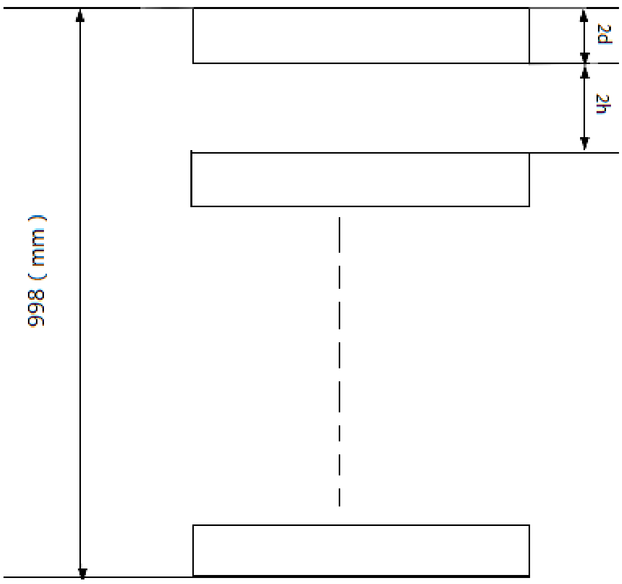

Figure 18: The dimension of the straight baffles with no angles

Number	d(m)	The air channel distance h(m)
8	0.025	0.04175
10	0.025	0.0275
12	0.025	0.0175

Table 5: The dimension of different straight parallel baffles mufflers.

S8_E and S8_H baffles mufflers

The S8_E and S8_H parallel baffles mufflers consist of eight MPP baffles, see Figure 19. The S8_H muffler contains the inner rigid walls, while S8_E muffler is empty inside. The dimensions of the mufflers can be checked in the Figure 18 and Table 5.

Figure 19: Photo of the parallel baffle mufflers S8_E and S8_H.

S10_E and S10_E

The S10_E and S10_H parallel baffles muffles consist of ten MPP baffles, see Figure 20 and table 5.The design of each of the baffles is similar to the previous case.

Figure 20: Photo of the parallel baffle mufflers S10_E and S10_H.

S12_E

The S12_E parallel baffles muffles consist of ten MPP baffles, see Figure 21 and table 5. All the baffles are without honey comb inside with same design as the previous cases.

Figure 21: Photo of the parallel baffle muffler S12_E.

3.2 The experimental results

3.2.1 The transmission loss of the tested mufflers

All the test samples are measured in the same experimental conditions. The experimental procedures followed are described in section two. The transmission loss for each muffler is tested at four flow speeds. The results are shown below.

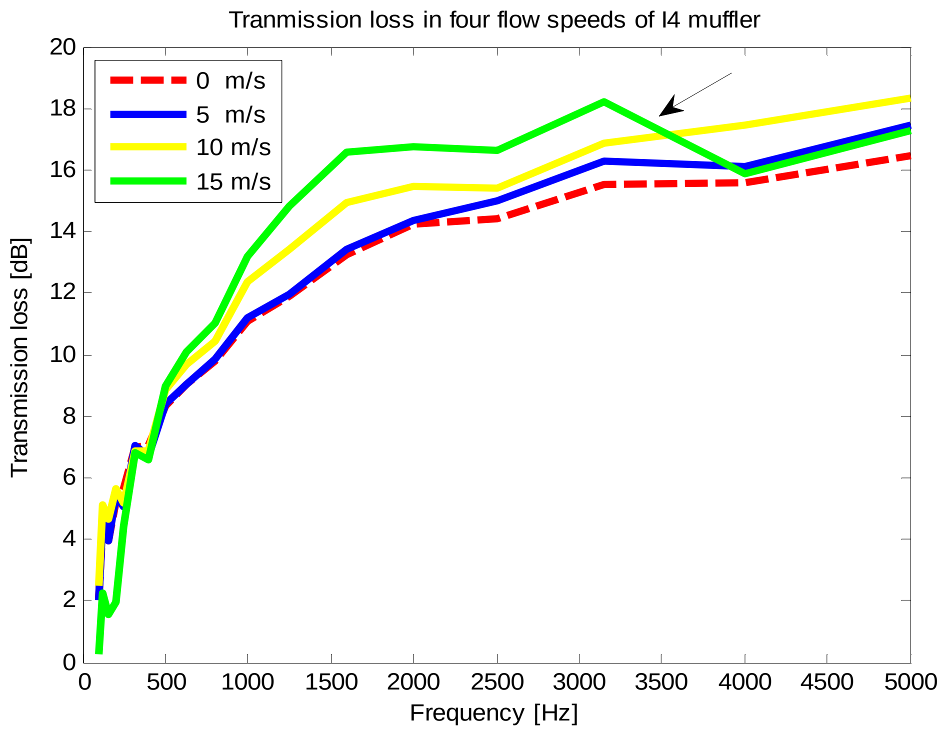

Figure 22: The transmission loss of the I4 parallel baffles muffler at different flow speeds.

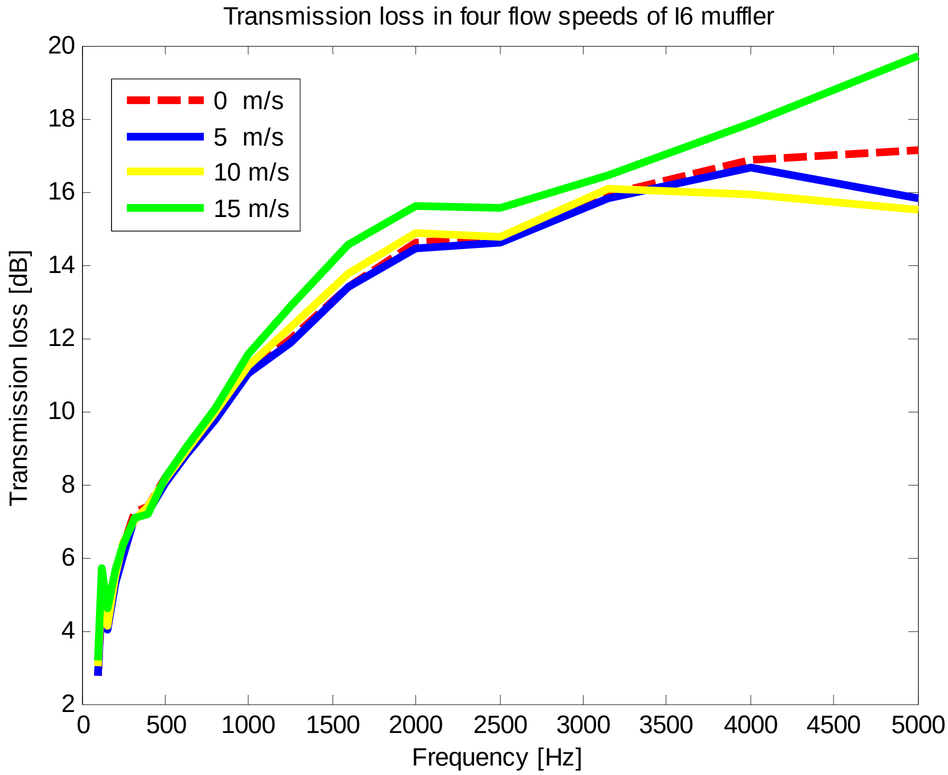

Figure 23: The transmission loss of I6 parallel baffles muffler at different flow speeds.

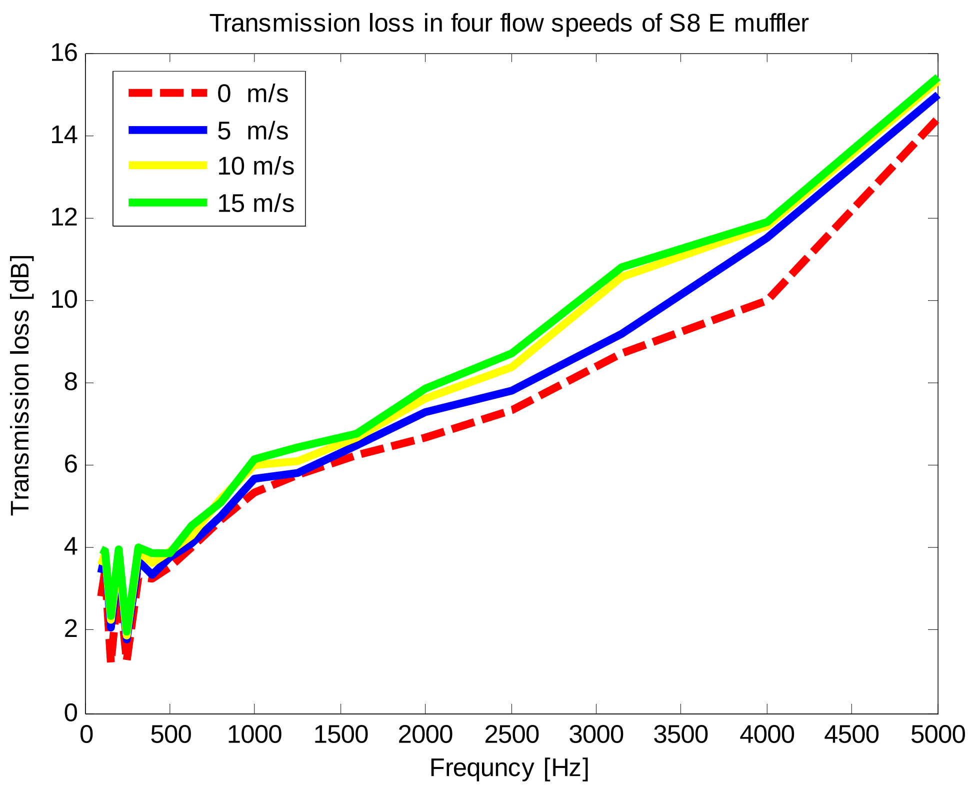

Figure 24: The transmission loss of S8_E parallel baffles muffler at different flow speeds.

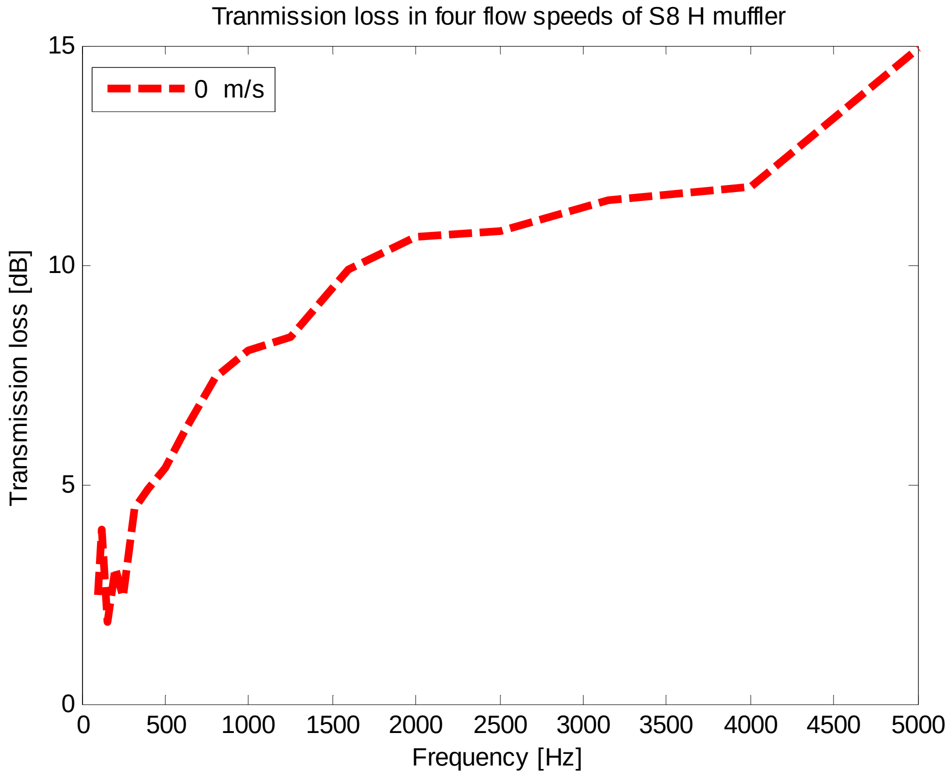

Figure 25: The transmission loss of S8_H parallel baffles muffler at zero flow.

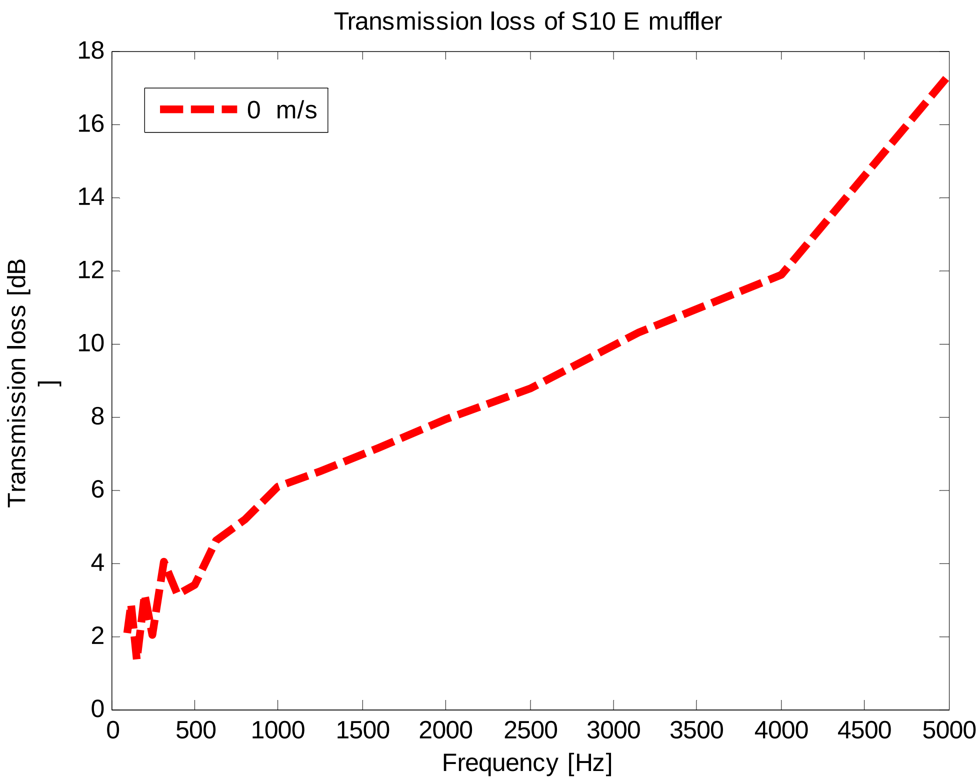

Figure 26: The transmission loss of S10_E parallel baffles muffler at zero flow.

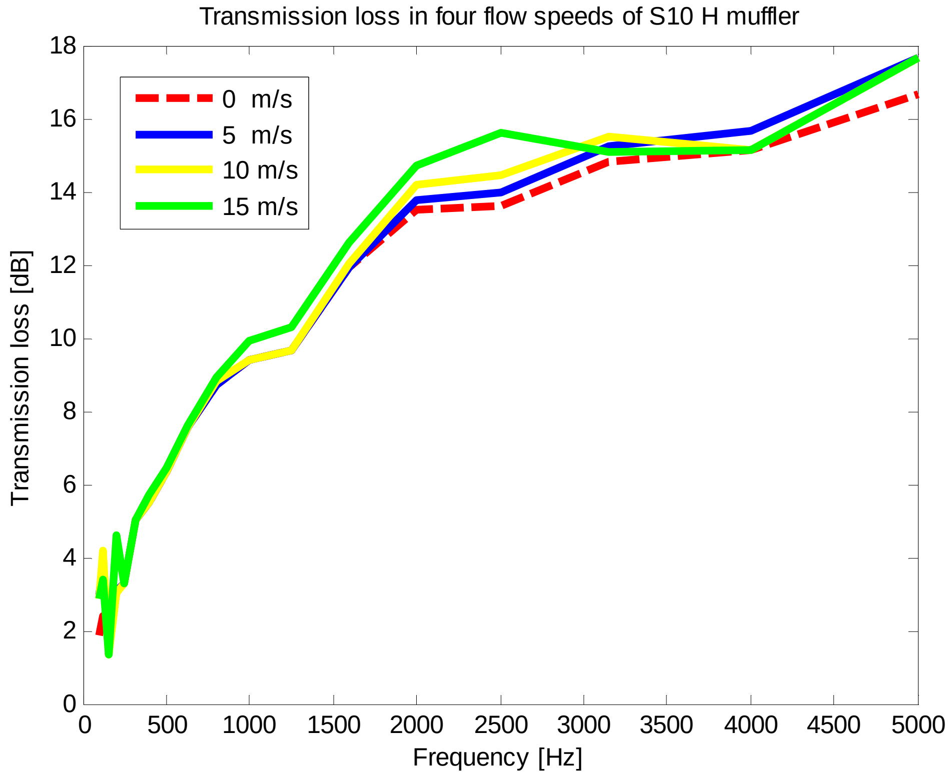

Figure 27: The transmission loss of S10_H parallel baffles muffler at different flow speeds.

Figure 28: The transmission loss of S12_E parallel baffles muffler at different flow speeds.

From all the experimental results, it can be concluded that the transmission loss increases with frequency but is weakly dependent on flow speed. Typically the transmission loss increase with less than 2-3 dB for the case tested and in practice this effect can be neglected. The effect can be explained by the increase in MPP resistance due to grazing flow [2]. From the experimental results it also can be observed that the transmission loss in the low frequency range is easier disturbed. Because, in the process of the experiment, the door of the reverberation room was kept open to evacuate the flow entering the room. This leads to some unwanted background noise in the low frequency range. Another problem for low frequencies is the small size of the test object, which gives so called "edge effects", i.e., the shape and size of the test object are causing a disturbance on the incident wave pattern creating deviations from the diffuse field assumptions.

3.2.2 The flow noise (ISO 3746:1995)

The muffler itself will create flow generated sound which was measured at the outlet of the muffler. The measured flow noise of the different mufflers are shown below.

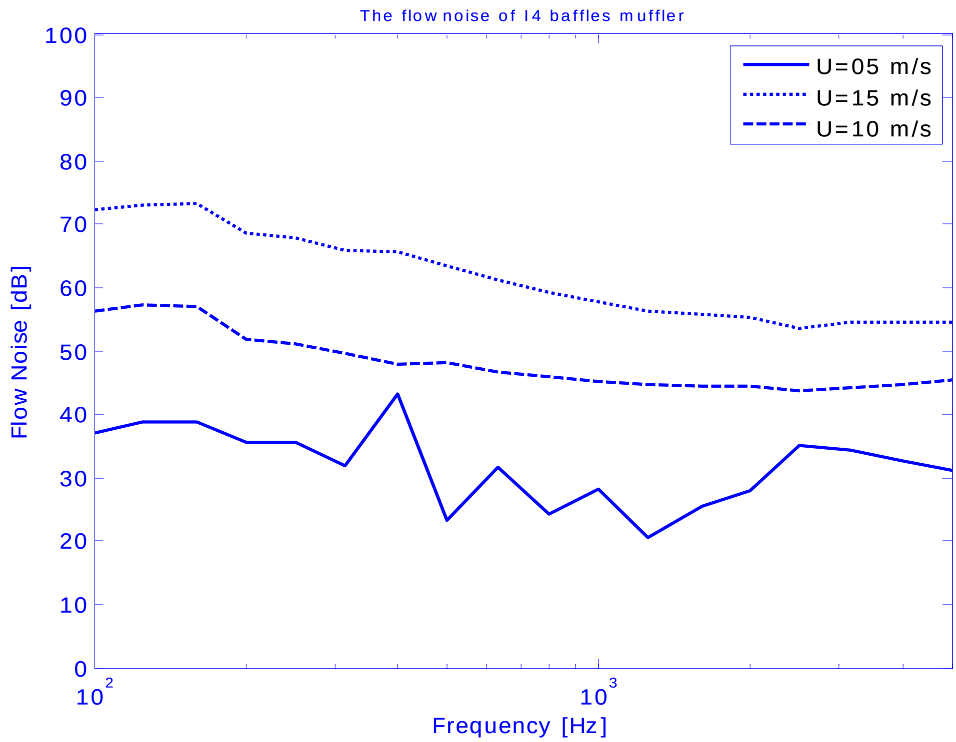

Figure 29: The flow noise of the I4 baffles muffler.

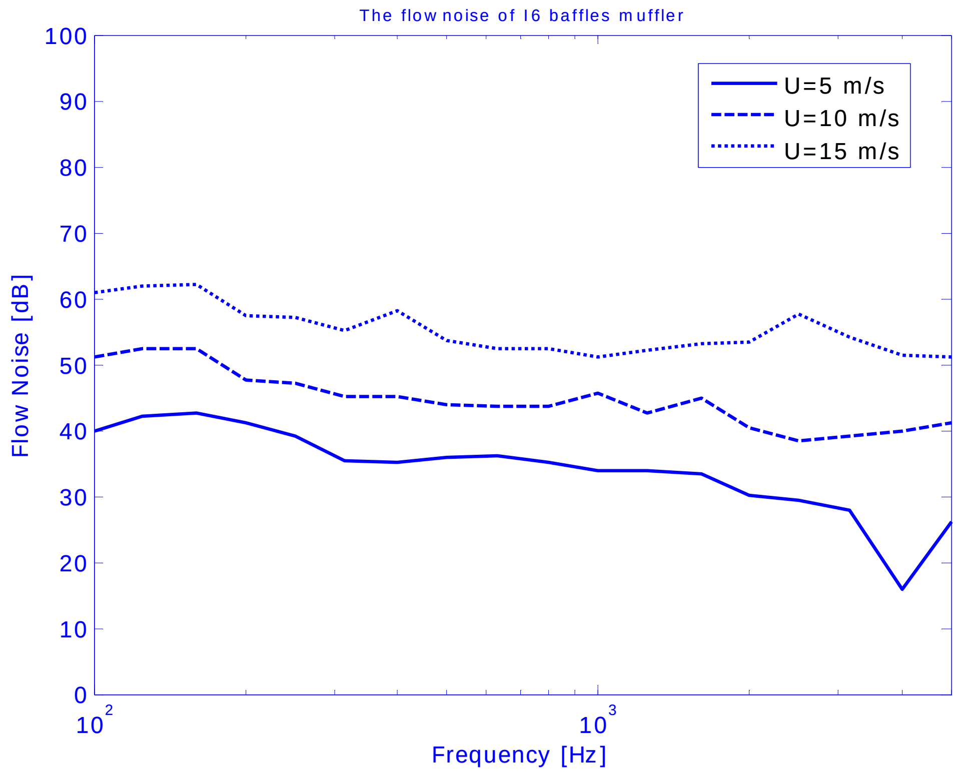

Figure 30: The flow noise of the I6 baffles muffler.

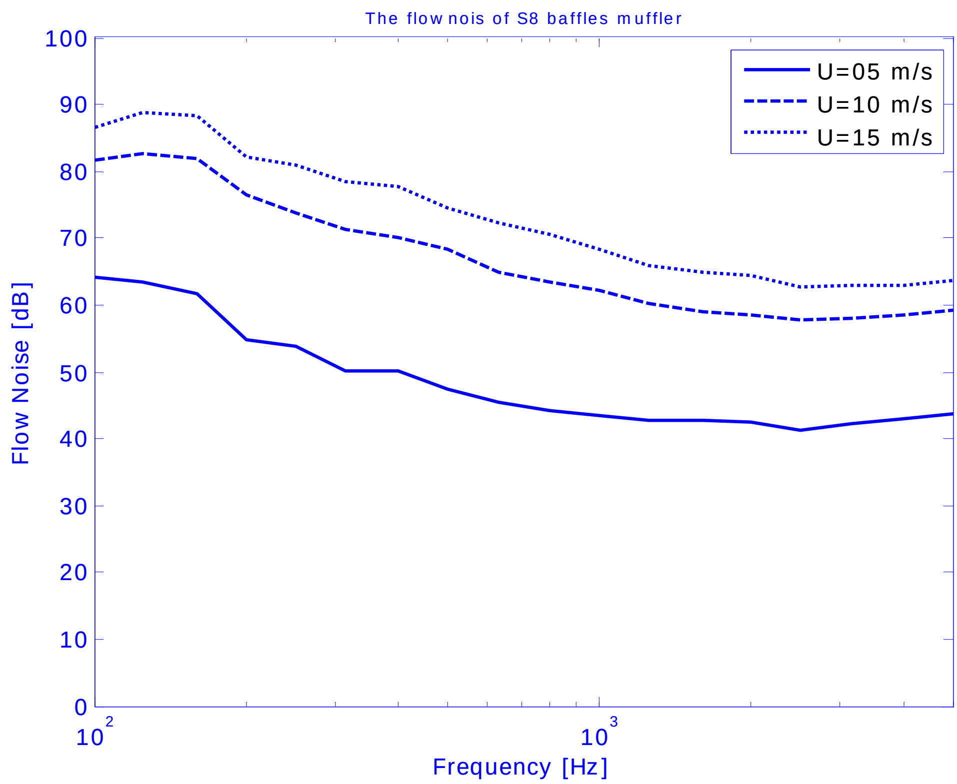

Figure 31: The flow noise of the S8 baffles muffler.

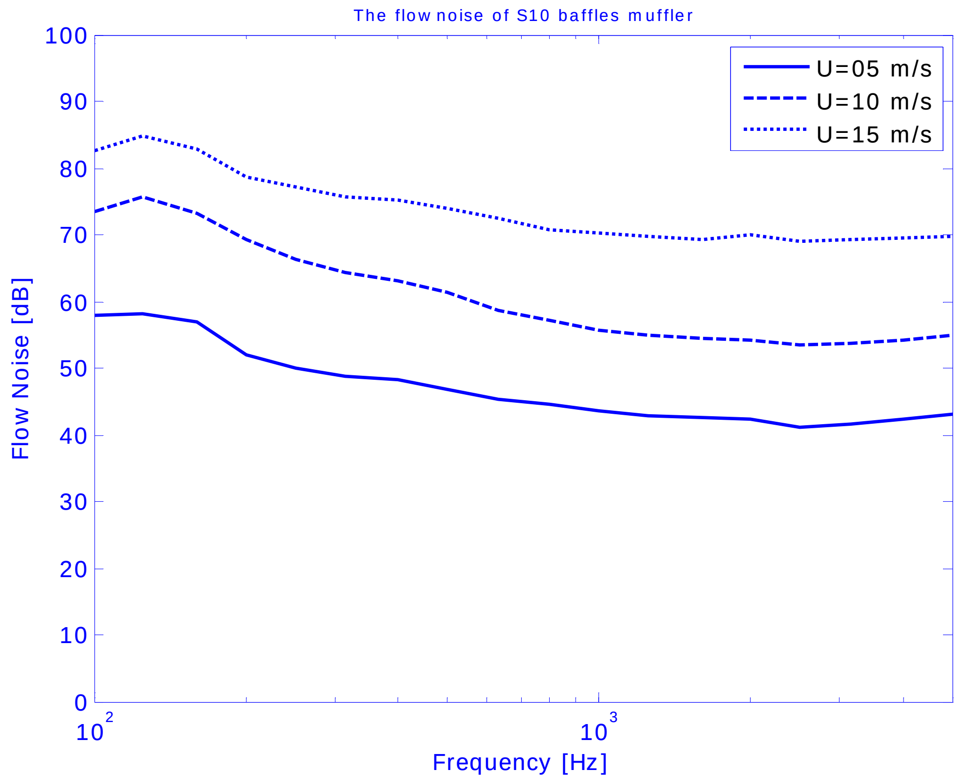

Figure 32: The flow noise of the S10 baffles muffler.

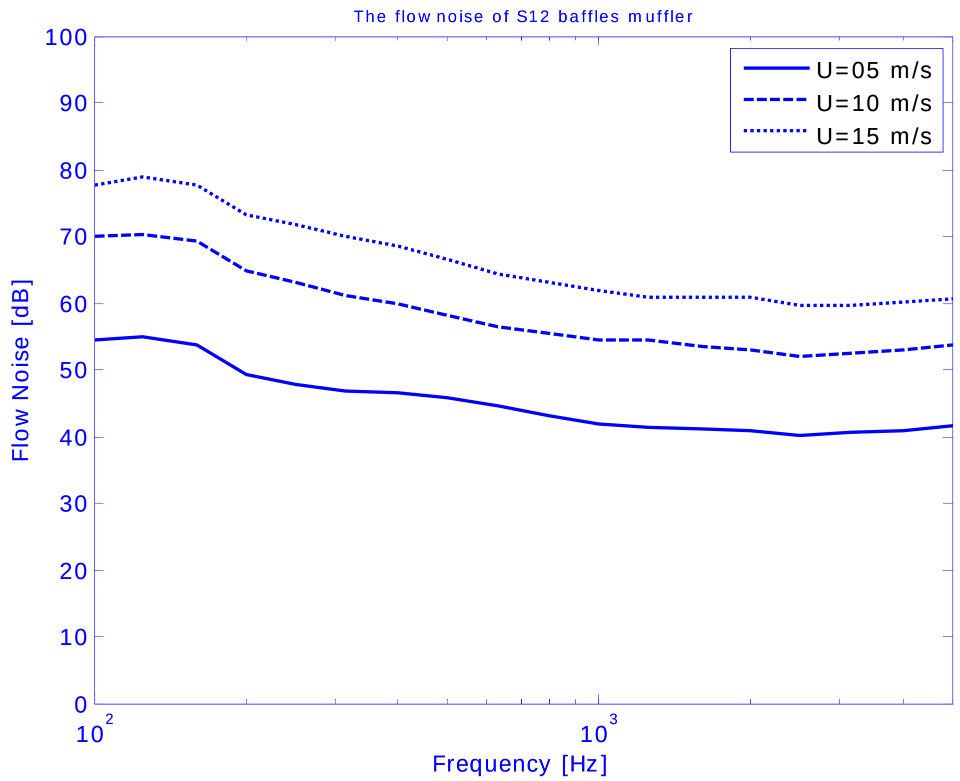

Figure 33: The flow noise of the S12 baffles muffler.

From the Figure 29 to 33, it can be seen that the flow noise is increasing with the flow speeds. The higher flow speeds will generate more flow noise by itself. The flow noise is affected by the baffles number and fixing angles. With increasing velocity 5m/s, the flow noise increase less than 8-15 dB for the case test. This can be explained that increasing the velocity will increase the sound power. Increasing the inclination and the baffles number will make more flow separation and this separation generates more noise approximately from 5-10 dB.

3.2.3 The comparison of different test samples

3.2.3.1 The comparison of transmission loss

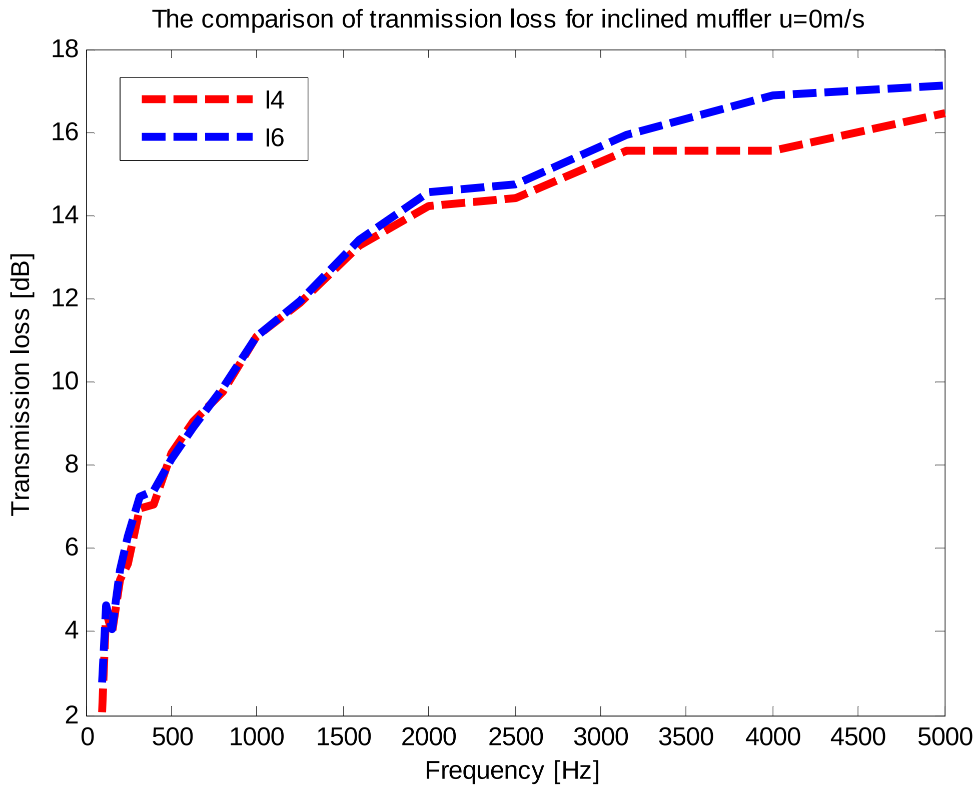

Figure 34: The comparison between the I4 and I6 mufflers without flow.

The I4 and I6 parallel baffles muffler consist of same baffle types. But they are fixed at different inclined angles, see Figures 15 and 17. From the Figure 34, it can be observed that the transmission losses of the I4 and I6 parallel baffles mufflers have no obvious differences in the low frequency range, below 1500Hz. And in the high frequency range, the transmission losses of the I6 muffler are slightly higher than the I4 muffler. It can be explained by the fact that the bigger inclined fixing angle, will lead to more reflections against the MPP walls for an incident wave.

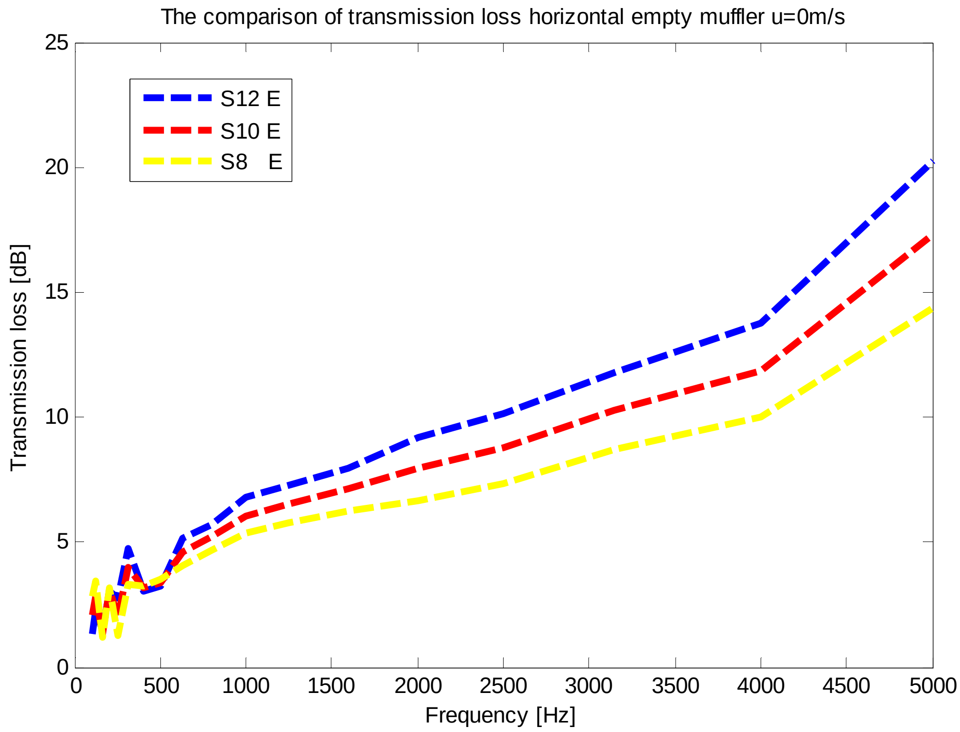

Figure 35: The comparison between the S8_E, S10_E and S12_E muffler.

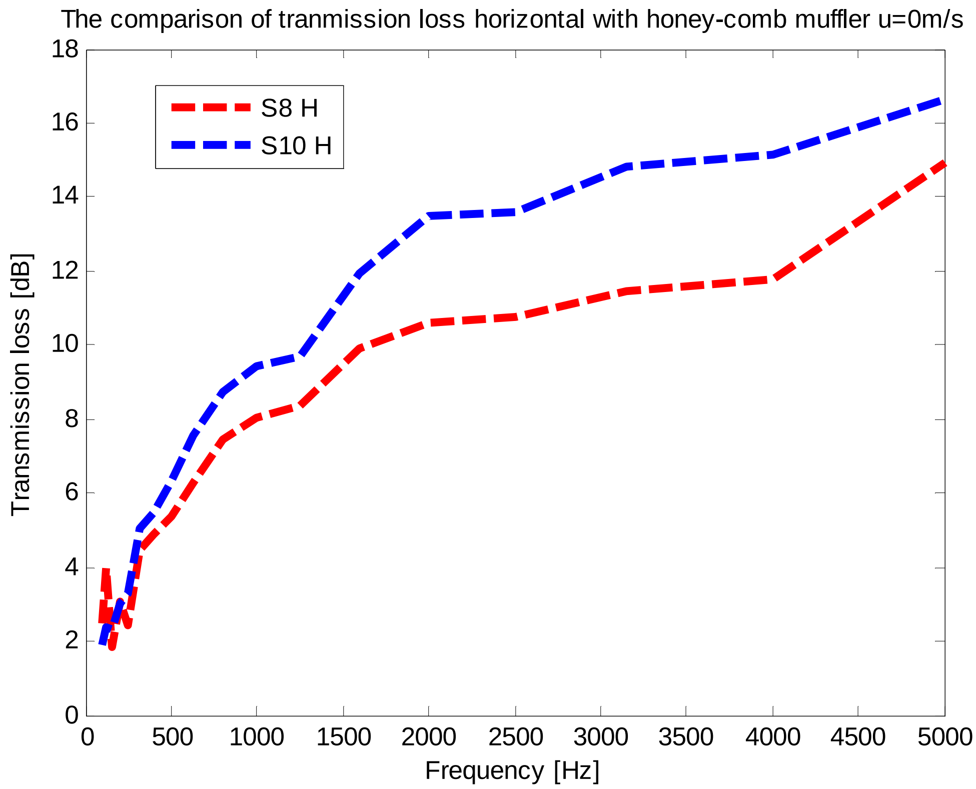

Figure 36: The comparison between the S8_H and S10_H muffler without flow.

From the Figure 35 and 36, it shows that increasing the number of baffles can increase the transmission loss.

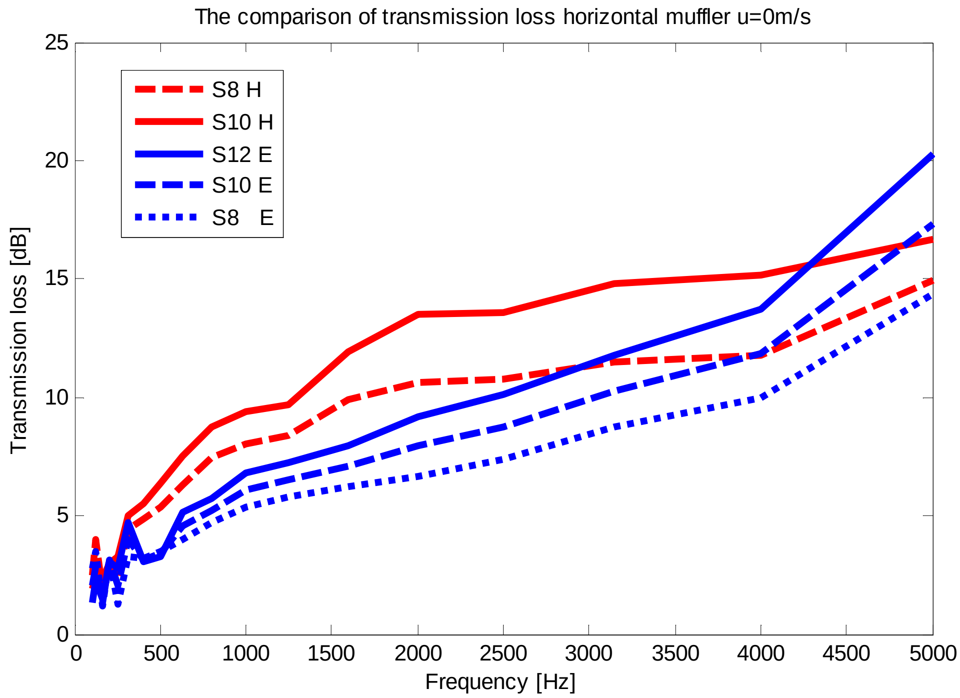

Figure 37: The comparison of horizontal parallel baffles.

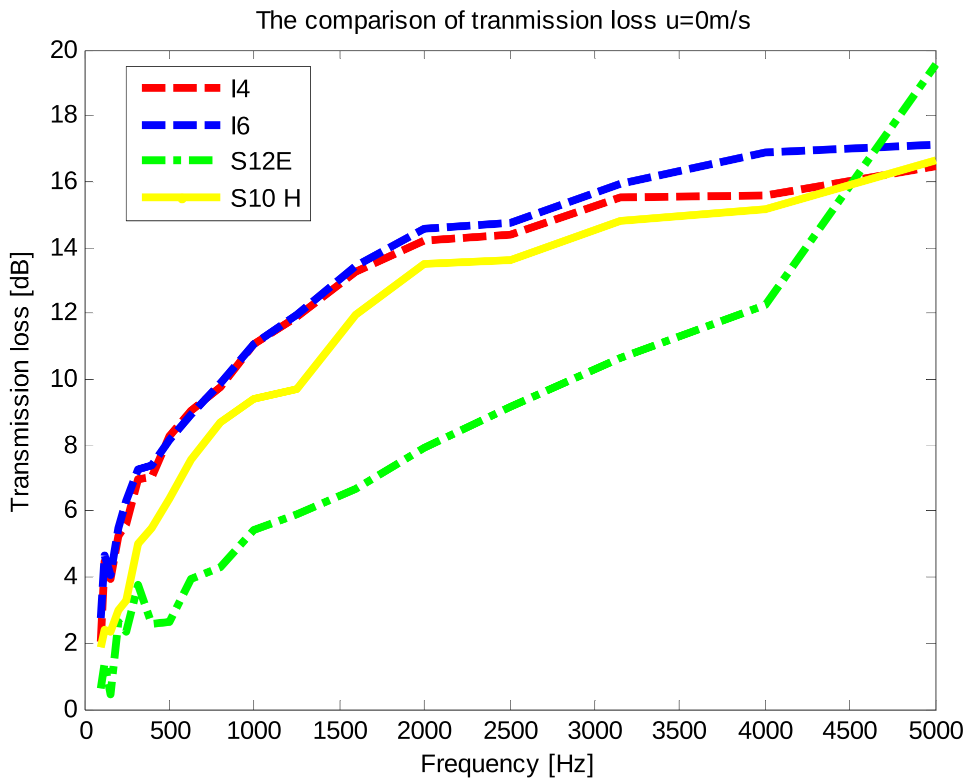

Figure 38: The comparison between the S10_H, S12_E, I4 and I6 muffler without flow.

From the Figure 37 and 38, it can be concluded that the transmission loss will be affected by the number of the baffles, the honey-comb inside and the fixing angle. A larger number of baffles will increase the transmission loss. The inner rigid walls ("honey-comb") can increase the transmission loss in particular in the low and mid-frequency range which is important. .

3.2.3.2 The comparison of flow noise

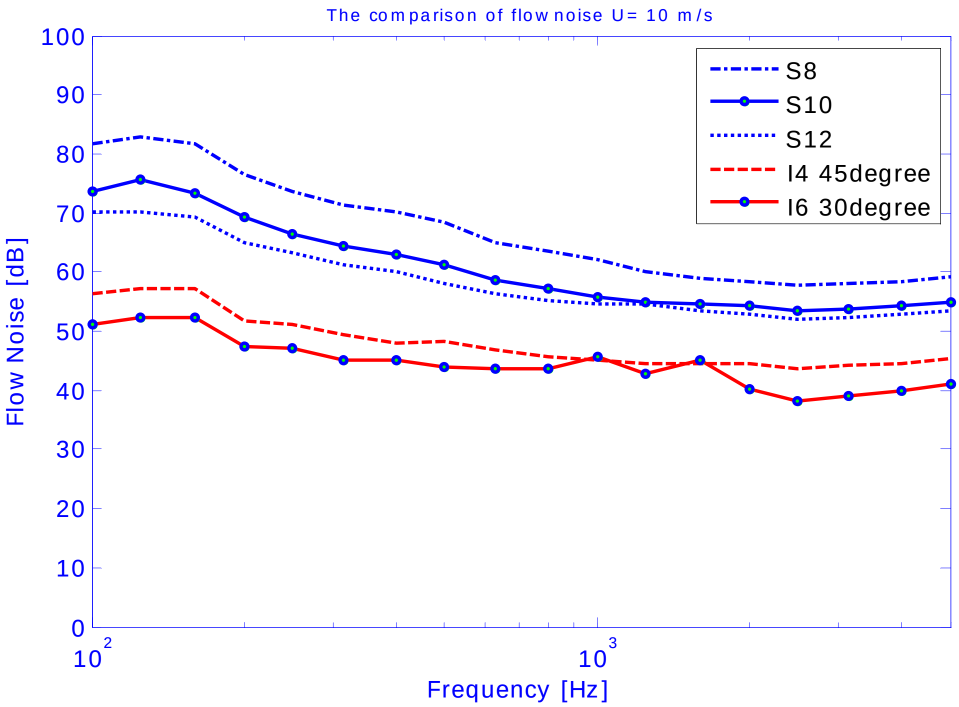

Figure 39: The comparison between the S10_H, S12_E, S8_E , I4 and I6 muffler with flow speeds 10 m/s

From the Figure 39, it can be concluded that the flow noise are affect by the number of the baffles and the fixing angle. More baffles inside the muffler will increase the flow noise and a larger inclination angle will increase the flow noise.

3.2.4 Pressure drops

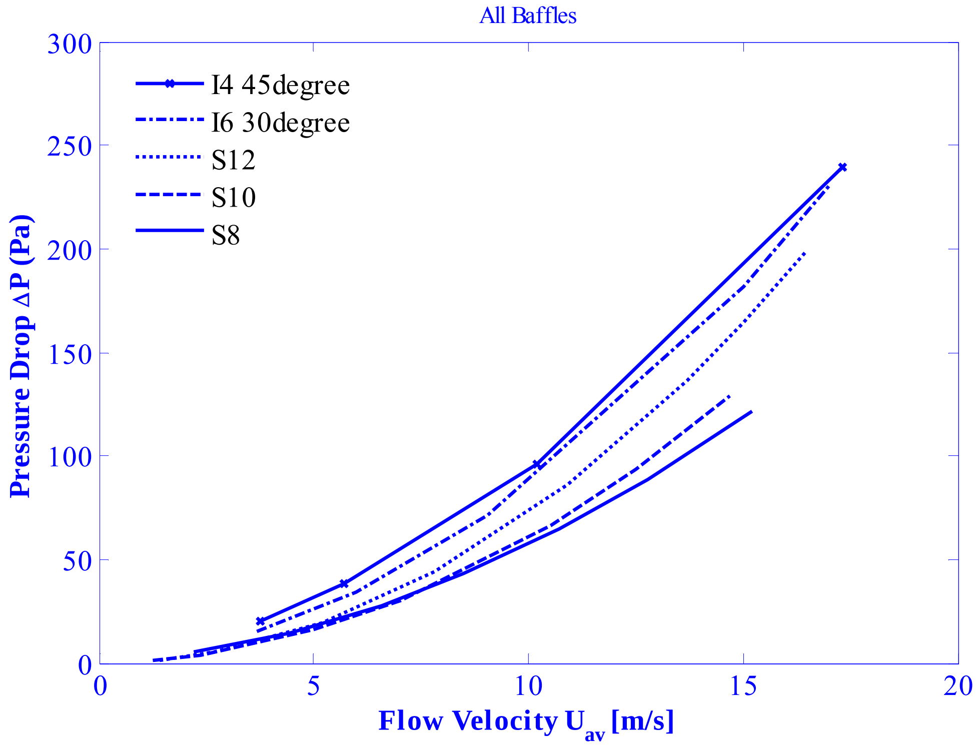

Figure 40: The pressure drop of the different mufflers.

From the Figure 40, it can be concluded that the pressure drop will be affected by the velocity, the number of the baffles and the fixing angle. With increasing the flow velocity, the pressure drop will increase. The inclination will lead to more pressure drop. And a larger number of baffles will increase pressure drop.

4. Models of parallel baffles muffler with locally reacting wall impedance

4.1 The geometry of the model

The parallel baffles muffler consists of a numbers of rectangular baffles, which in our case are made of Micro-perforated panels. In the model used here it will be assumed that the baffles are filled with rigid inner walls separated by distance much smaller than a wavelength. The baffle surface can then be assumed to be locally reacting [7, 8]. The whole structure of the muffler is shown in Figure 41. The separation of two baffles is 2H. Every two adjacent half baffles build up a single channel which is the basis for the model, which can be observed in the Figure 42. The length D is the half width of a baffle.

The coordinate system is built on the whole structure of the muffler as shown in Figure 41. The sound propagates along the z direction. And Figure 46 shows the passages of the sound, along the baffles, which is the yz surface in Figure 43.

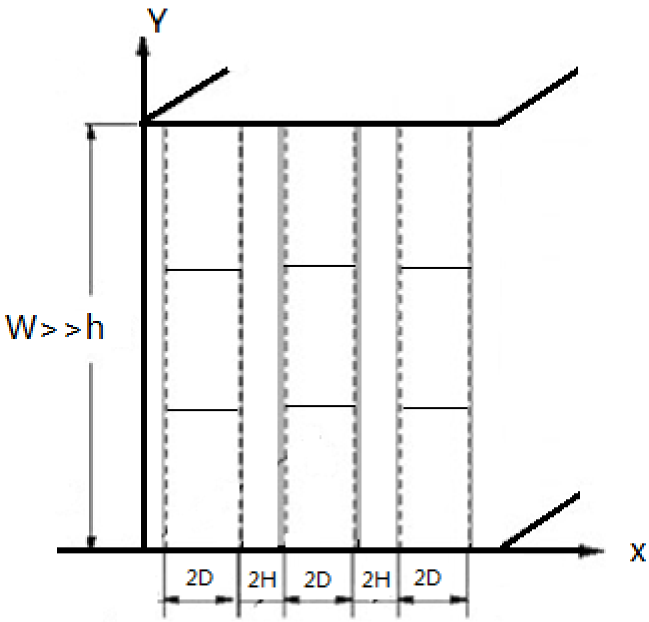

Figure 41: The structure of parallel baffles muffler.

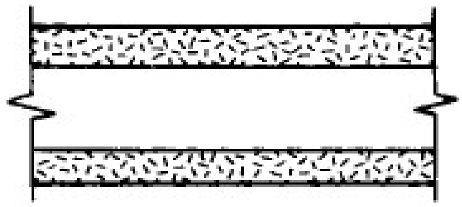

Figure 42: The structure of a single baffle channel used in the mode [11].

4.2 The theoretical formulation of the model:

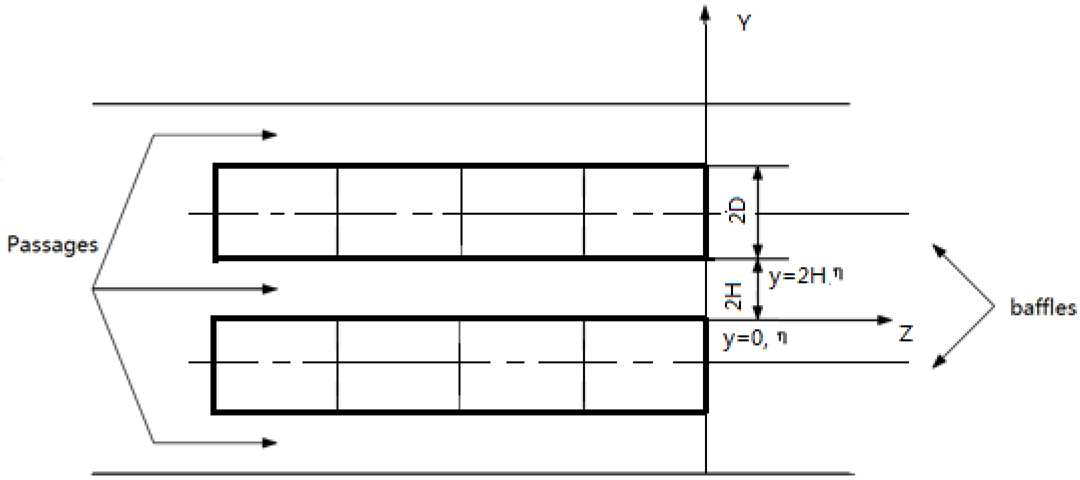

Figure 43: The simplified single channel model [7, 8].

Assumption of the wave propagation along the z-axis in the form of modes over the cross-section [8] with harmonic time (e^{iwt}) dependence gives:

$$p(z, y, \mathrm{x}, \omega) = \left[A \cdot \cos(k_Y \cdot y) + \mathrm{B} \cdot \sin(k_Y \cdot y)\right] \cdot \cos(k_x \cdot x) \cdot e^{-ik_z Z}$$
$$= A \cdot \left[\cos(k_Y \cdot y) + \mathrm{R} \cdot \sin(k_Y \cdot y)\right] \cdot \cos(k_x \cdot x) \cdot e^{-ik_z Z}$$

$$k_Z^2 + k_y^2 + k_x{}^2 = k_0^2 = \left(\frac{\omega}{c_0}\right)^2 \qquad (10)$$

Note only symmetric modes are considered in the x-direction and here we will simply assume that k_x=0.

The equation of motion in the y-direction gives：

$$\rho \frac{\partial u_y}{\partial t} = -\frac{\partial p}{\partial y}$$

$$\rho \cdot i \cdot \omega \cdot u_y = \text{-}A \cdot \mathrm{k}_y \cdot \left[-\sin(k_y \cdot y) + R \cdot \cos(k_y \cdot y)\right] \cdot \cos(k_z \cdot x) \cdot e^{i \cdot k \cdot_z z}$$

$$\frac{u_y}{p} = \frac{k_y}{\rho \cdot i \cdot \omega} \cdot \frac{\sin(k_y \cdot y) - R \cdot \cos(k_y \cdot y)}{\cos(k_y \cdot y) + R \cdot \sin(k_y \cdot y)} = \frac{\eta}{\rho \cdot c}$$

Where the admittance is defined at the MPP wall surface (y=0/2H) which is assumed locally reacting.
Again only considering symmetric modes now in the y-direction leads to the following equation for the wave numbers in the y-direction:

$$K_y \cdot \tan(K_y \cdot k \cdot 2\mathrm{H}) = \frac{i \cdot (\eta_1 + \eta_2)}{1 + \frac{1}{K_y^{\;2}} \cdot \eta_2 \cdot \eta_1} = i \cdot \frac{2\eta}{1 + \frac{1}{K_y^{\;2}} \cdot \eta^2} \tag{11}$$

Where Ky=k_y/k, and k=ω/c.

The complex axial wave number, Ky, can be solved from equation (11), which is a transcendental equation, by the means of the Newton-Raphson method [10].

Once the wave numbers across the duct are given the propagation wave number Kz can be calculated by the following equation:
$Kz= (K_0^2-Ky^2-Kx^2)^{1/2}$ (12)
where in our case Kx=0 is assumed and Ko is equal to ω/c.

The impedance of a micro-perforated panel can be computed by the model suggested by Ma [2] with flow effects added by Guo et al. [1]. Using these formulas and adding the impedance of an air cavity with the height D gives the admittance needed in the above model. The data for the MPP plates used was taken from the measurements in Ref. [1] which were done on the same plates, see Figure 44.

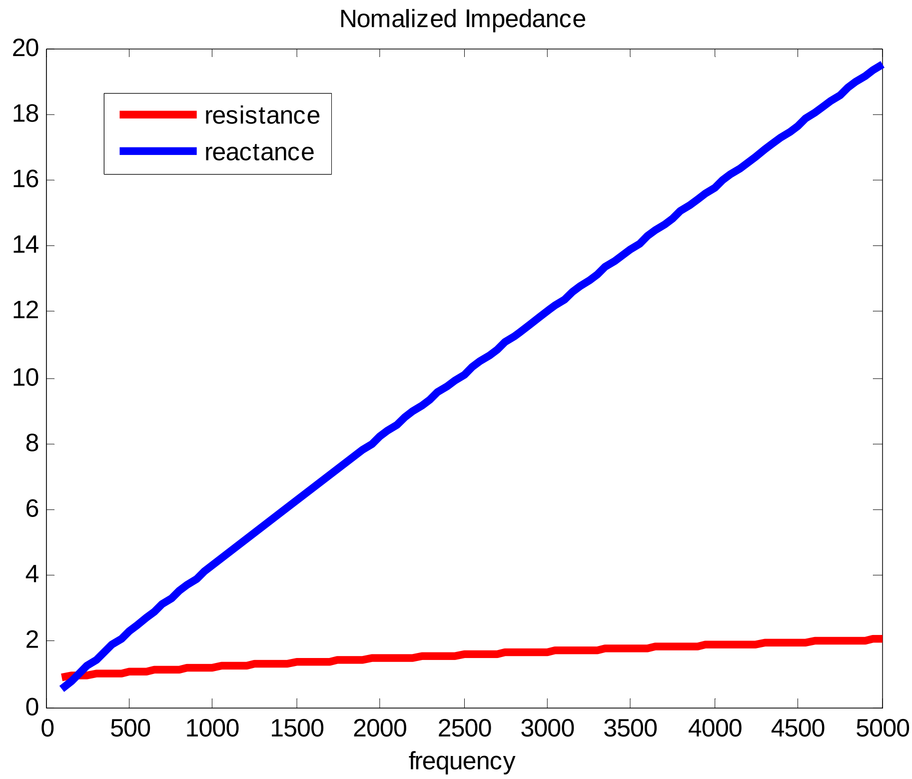

Figure 44: The impedance of the MPP used (Acustimet^{TM}).

4.3 The modeling results

4.3.1 The transmission loss

Figure 45 shows the computed transmission loss for the lowest mode, i.e., the first solution to the transcendental equation. The transmission loss is computed only based on the damping along the baffle, i.e., using the imaginary part of the Kz wave number. That is the reflections at inlet and outlet are neglected.

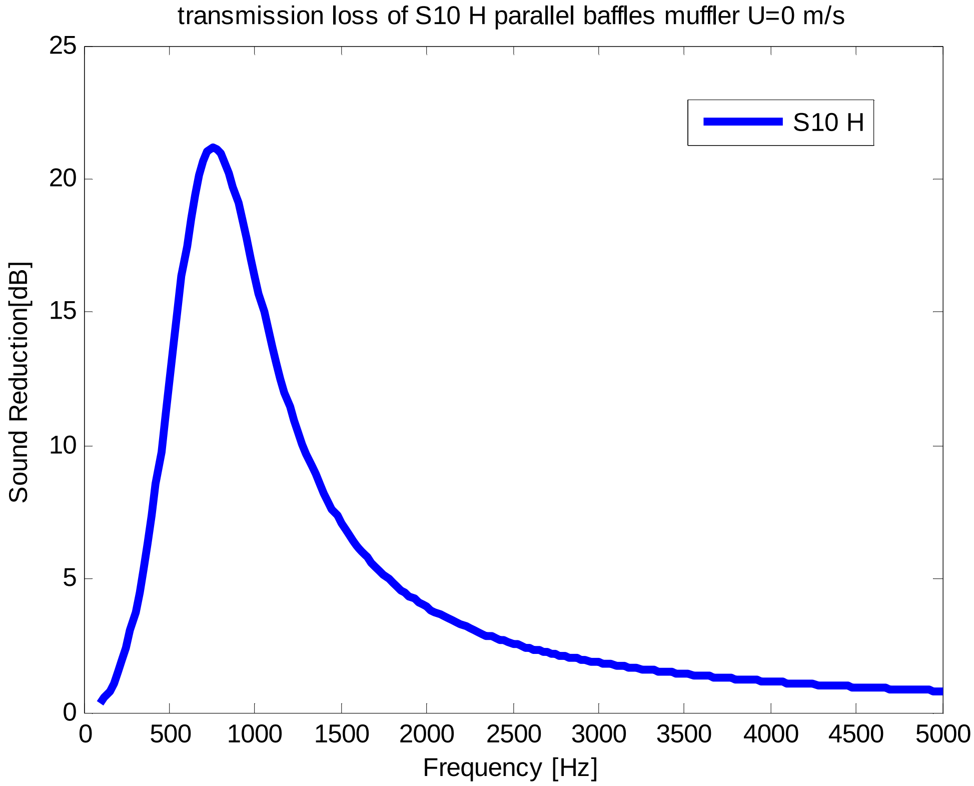

Figure 45: The transmission loss of the S10_H parallel baffles muffler U=0 m/s.

Figure 46 shows the predicted increase in transmission loss from increasing the baffles from 8 to 10.

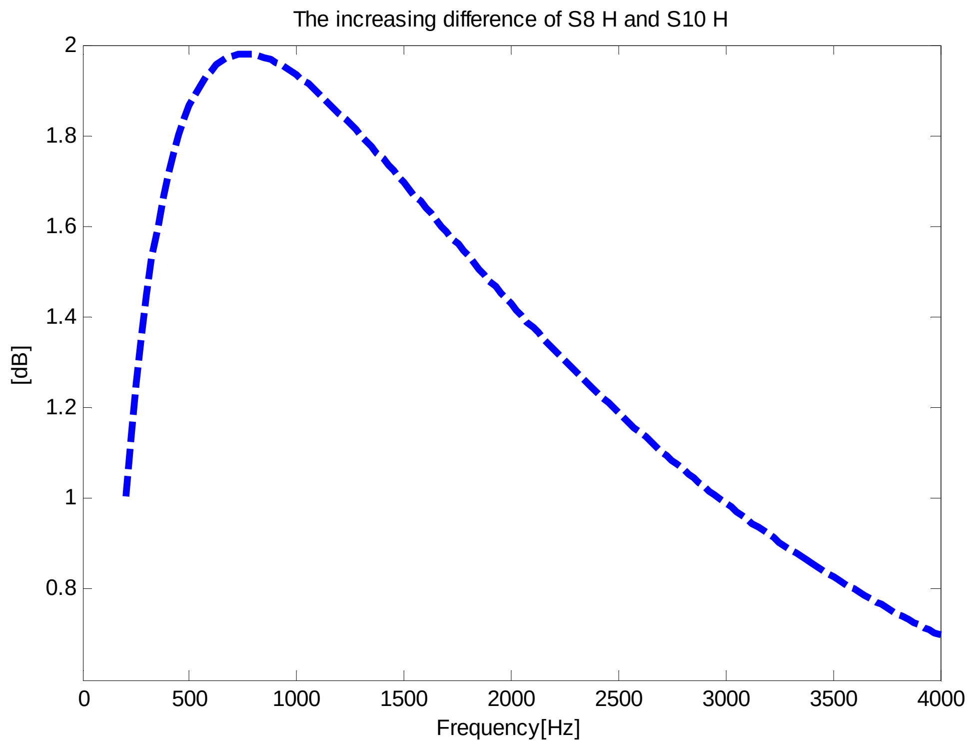

Figure 46: The transmission loss of the S10_H parallel baffles muffler U=0 m/s.

4.3.2 The comparison of modeling and experiments

Below the calculated and measured transmission loss is plotted for a few cases. As can be seen there is a large difference related to the fact that the model only considers one mode and in the experiments we have a number of modes and are measuring the average. To improve the comparison one should therefore compute more modes and compute an average.

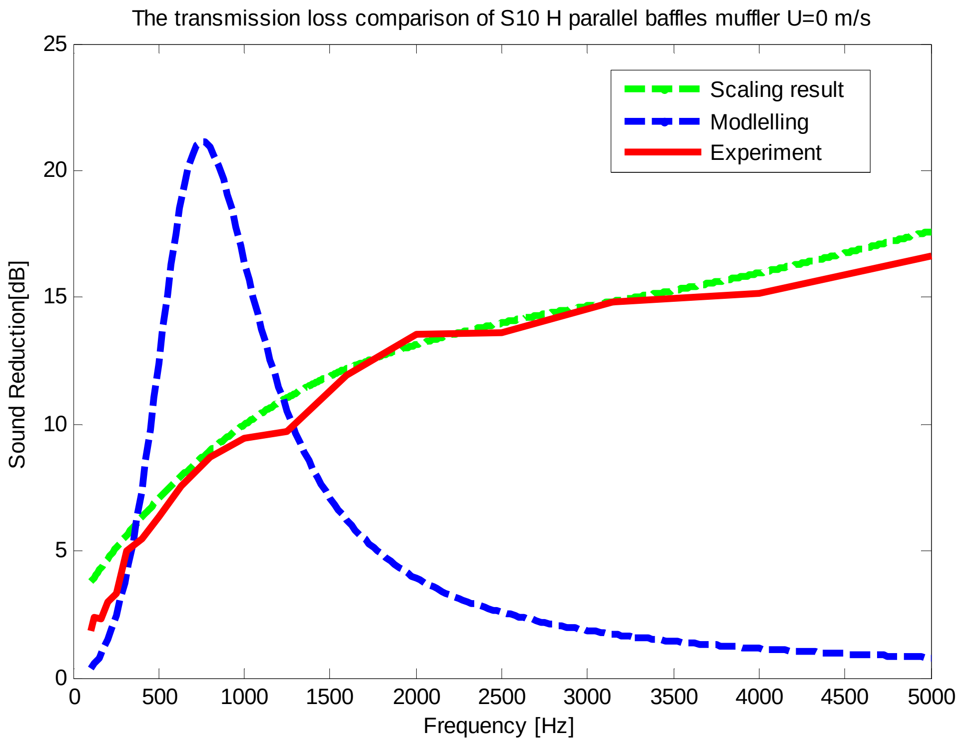

Figure 47: The transmission loss of the S10_H parallel baffles muffler U=0 m/s.

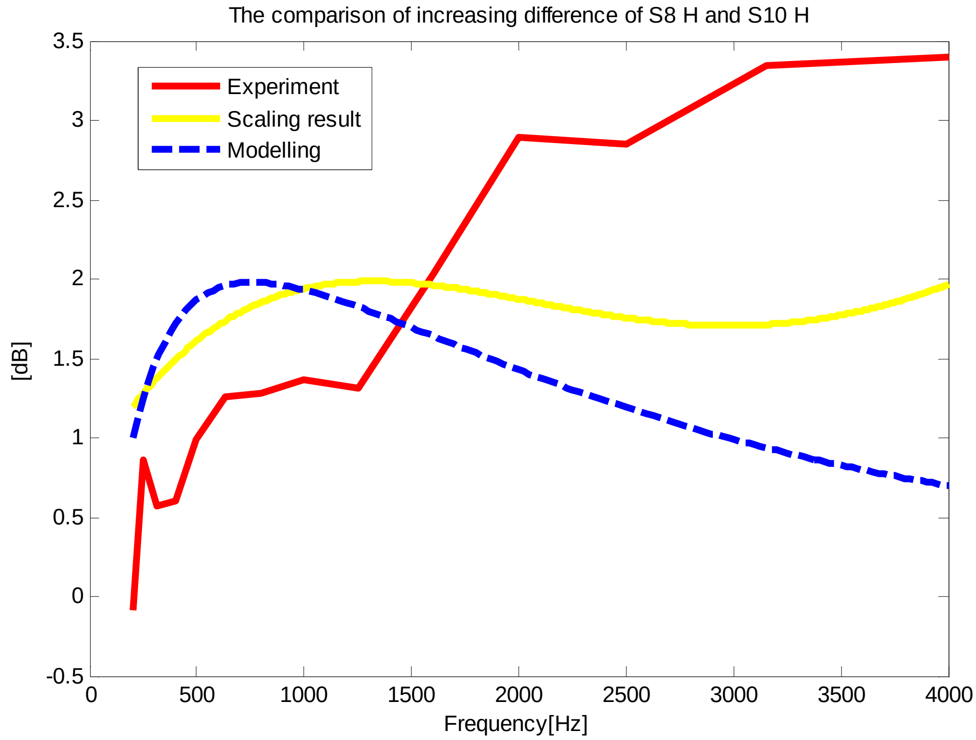

Figure 48: The difference between the S10_H and S8_H muffler transmission loss.

5. Summary and conclusions

The transmission loss and flow-generated sound have been investigated for seven kinds of parallel baffles mufflers. It is found that the transmission loss can be enlarged by increasing the number of baffles, adding the inner rigid walls inside the baffle and using inclined baffles. The inclined baffles mufflers with inner rigid walls have the largest transmission loss. The inclination increases the high frequency performance while the inner rigid walls give an increase for the low and mid frequency range. The flow-generated sound is affected by the number of baffles and the inclination angle. Increasing the number of baffles and increasing the inclination angle will increase the flow noise.

The model of the horizontal parallel baffles muffler with inner walls is based on locally reacting liner theory. The calculated results presented are only for the lowest mode and cannot therefore be directly compared with the experimental results. A more complete model should be based on average transmission loss computed for a number of modes.

References

(1) D.-Y Maa. *Potential of microperforated panel absorber*, J. Acoust. Soc.Am., vol.104, no.5, November

(2) Ying Guo, Sabry A., Åbom M., *Micro-Perforated Plates for Vehicle Applications* 37th International Congress an Exposition on Noise Control Engineering 26-29 October 2008. Shanghai. China

(3) 15186-1:2000 *Acoustics- Measurement of sound insulation in building and building elements using sound intensity*- Part 1: Laboratory measurements.

(4) Leping Feng *Acoustic Measurements,* Chapter 5&10. KTH, The Royal Institute of Technology, The Marcus Wallenberg Lab., Stockholm, TRITA-AVE2007:07, ISSN 1661-7660, 2008.

(5) Åbom M, Yan J., *Acoustic Modeling of Heat Exchangers* 37th International Congress an Exposition on Noise Control Engineering 26-29 October 2008.Shanghai. China

(6) M.L. Munjal*. *Analysis and Design of Pod Silencers* Journal Sound and Vibration 262 (2003) 497- 507.

(7) A.G. Galaitsis, I.L. Ver, *Passive silencers and lined ducts*, in: L.L. Beranek, I.L. Ver (Eds.), Noise and Vibration Control Engineering, Wiley-Interscience, New York, 1992 (Chapter 10).

(8) Uno Ingard, *Noise Reduction Analysis (Physics),* Jones&Bartlett Publishers, 2009 (Chapter 6&10).

(9) M. Åbom, *An Introduction to Flow Acoustics*. KTH, The Royal Institute of Technology, The Marcus Wallenberg Lab., Stockholm, TRITA-AVE2006:04, ISSN 1651-7660, ISRN KTH/AVE/N-06/04-SE, 2006.

(10) Z.C. Qi, *Numerical Analysis*. National Defense University of science and technology Publishers, Beijing, 1987.

(11) M.L. Munjal, *Acoustics of Duct and Mufflers*, Wiley- Interscience, New York, 1987.

(12) HP Wallin, U Carlsson, M Åbom, H Bodén and R Glav *Sound and Vibration*. KTH, The Royal Institute of Technology, The Marcus Wallenberg Lab., Stockholm, ISSN 978-91—7415-553-2, 2001.